YTUP

Journal of Thermal Engineering

https://jten.yildiz.edu.tr/

https://doi.org/10.47481/jten.0005

RESEARCH ARTICLE

Comparison of piezoelectric fans with different geometries

Mehmet Onat Mormenekşe[1,*], Mehmet Özdemir[2], Ayhan Onat[3]

[1]Marmara University Institute of Pure and Applied Sciences, Mechanical Engineering, Maltepe, İstanbul, 34854, Türkiye
[2]Marmara University Institute of Pure and Applied Sciences, Mechanical Engineering, Maltepe, İstanbul, 34854, Türkiye
[3]Marmara University, Faculty of Technology, Mechanical Engineering, T3-310, Maltepe, İstanbul, 34854, Türkiye

Abstract

The continuous miniaturization of electronic devices makes conventional rotary fans widely adopted in electronic systems, less practical due to their space requirements and undesirable noise generation. Hence, piezoelectric fans have attracted much attention as an alternative cooling solu-tion, due to their compact structure, silent operation and relatively low energy consumption. In this work, the cooling performance of various configurations of piezoelectric fans are investigated with special attention to the influence of blade geometry and material choice on the thermal per-formance. Different configurations using PZT-4 piezoelectric ceramics and various blade and actuator materials were experimentally tested. Results show that the generation of airflow and the cooling capacity are highly sensitive to the blade structure design and the materials selected. The best overall performance was obtained for a stainless-steel blade design with optimized geometric characteristics, which offered a temperature decrease of 9.89 °C at a power consumption of just 22.64 mW. And wider blade geometries provided better air flow distribution and cooling effi-ciency than narrower blades. The choice of materials also played a key role in the performance of the actuators, with the bronze actuators outperforming the copper ones. The results indicate the close relationship between material properties, structural flexibility and geometric design in the effectiveness of piezoelectric fans. The piezoelectric coolers have advantages in size and energy efficiency, but the integration of these coolers in electronic assemblies needs careful evaluation to avoid possible vibration-related interactions or interference.

Keywords: Piezoelectric fans; electronic cooling; thermal management; blade geometry; pzt-4 ceramics; actuator materials; vibration interference

Cite this article as: Mormenekşe, M. O., Özdemir, M., & Onat, A. (2026). Comparison of piezoelectric fans with different geometries. Journal of Thermal Engineering, 12(3), 2–10. https://doi.org/10.47481/jten.0005

1. Introduction

A significant portion of malfunctions in electronic devices originates from the inability to manage the excessive heat generated during their operation. In such complex systems, traditional air-cooling methods can be challenging to implement due to limited working space. Moreover, miniaturization of conventional rotary fans often leads to reduced energy efficiency (higher power consumption). In recent years, piezoelectric fans have emerged as an alternative solution.

While regular fans are often bulky and take up a lot of space, piezoelectric fans are much smaller. By getting rid of heavy mechanical parts, they offer a much thinner and smoother design. They're also a go to for quiet settings because they operate with far less noise than their motor driven counterparts.

These innovative cooling tools work by converting electrical charge into mechanical vibrations, creating a steady airflow without the need for traditional motors. While their efficiency and near silent operation make them a compelling alternative to standard fans, their actual performance is deeply tied to material properties and specific design choices. This makes it essential to evaluate how different fan geometries impact heat dissipation if we want to push this technology further.

Recent breakthroughs in piezoelectric cooling have branched into two main areas: structural innovation and driver integration. Research by Abdul Razak et al. on radial configurations (RPMF) underscores how much geometric fine-tuning can improve heat transfer [1]. As a complement, the "brain" of the system has been the object of the work of Yang et al., who built power-efficient driving methods that reduce power loss

*Corresponding Author
E-mail Adress: mo.mormenekse@hotmail.com

Submitted: 18 October 2025; **Accepted:** 22 October 2025

This paper was recommended for publication in revised form by Editorin-Chief Ahmet Selim Dalkılıç

[2]. The studies show that in order to reach next generation performance a dual approach is required, addressing both the physical fan and the circuits behind it. Miniaturized systems, where space and noise are at a premium, can be poorly served by conventional cooling techniques. As a result, piezoelectric fans have become a promising alternative.

Traditional cooling methods often fall short in miniaturized setups where noise and space are at a premium. Consequently, piezoelectric fans have emerged as a promising alternative. This study examines the critical variables namely blade geometry and material selection that dictate how effectively these fans can dissipate heat. A total of 16 configurations were fabricated using PZT-4 ceramic three-layer actuators combined with blades of stainless steel and polyvinyl chloride (PVC). Each configuration was experimentally tested under identical conditions at the resonance frequency, with a 288 Vpp input. Our experiment reveals that cooling performance is heavily determined by the coordination between blade shape and actuator material. In particular, the best results were obtained with the stainless-steel fan with blade Type-B and bronze intermediate layer, with a temperature reduction of 9.89°C and a low power consumption of 22.64 mW. Efficiency is not a single factor but combination of stiffness, thermal conductivity and geometry. Although piezoelectric fans have been discussed in previous work, most of these have considered these variables in isolation. This study provides a unique, systematic perspective on how wider blade designs and bronze-based actuators actually can outperform traditional designs in compact or biomedical applications, by testing 16 different configurations side-by-side.

In essence, piezoelectricity is a reversible effect: these materials generate electricity when compressed and vice versa become deformed when an electric field is applied. This effect is caused by asymmetric orientation of atoms in the crystal matrix. Some materials, such as quartz, barium titanate and Lead Zirconate Titanate (PZT) are piezoelectric. When compressed or stretched, the internal dipoles align and create a measurable voltage. [3].

These materials serve three main functions: as sensors for monitoring variables such as acceleration and strain, as actuators for fine-tuned motion, and as harvesters for converting mechanical energy to power. This flexibility has made them indispensable tools in many areas, ranging from healthcare technology to the emerging field of wireless sensing.

Piezoelectric fans are so reliable because of the high resonance frequency compatibility and long-term durability. They need so little maintenance and have such a long service life that they are often a much more sustainable choice than traditional mechanical fans. [4].

In the presence of an electric field piezoelectric materials behave in two fundamental ways: they either increase in thickness or contract in their plane. This thickness expansion causes the bending motion in stack actuators. The other one uses bending type actuators. They are based on in-plane contraction, which causes lateral shrinkage, and are used to produce the necessary movement. These typically consist of a base layer and a PZT ceramic layer [5].

There are longitudinal displacement actuators and in-plane contracting actuators. In the former case, the electric field is applied along the poling direction of the ceramic layer. Although the deformation is small, stacked structures, mechanically in series and electrically in parallel, are developed to achieve sufficient displacement, enabling up to 0.10-0.15% elongation of the actuator's length. In-plane contracting actuators produce displacements perpendicular to the poling direction, enabling movements of up to 20 μm. Their multilayer structure allows operation at lower voltages and greater force output [6].

Bending behaviour occurs when in plane contracting actuators are fixed to a substrate. While you can build a fully ceramic bending element by pairing two active piezoceramic layers, using a passive substrate like metal or ceramic creates what is known as a composite bender. These piezoelectric arrangements are very pliable and can be made in single or multi-layer designs depending on the power needed. [6].

Since the first proposal of this concept by Toda in 1979, the research on piezoelectric fans has been promoted vigorously due to the urgent demand of new cooling solutions. Airflow is generated by the fans vibrating at their natural frequency due to an alternating current (AC). Earlier experimental results have reliably demonstrated large enhancements of heat transfer [7]. For instance, Kimber et al. discussed in detail the effect of geometric and material composition of the fan on its thermal efficiency. Both physical testing and numerical models of their results confirm that these fans are not only effective at surface cooling but are particularly well suited for high efficiency, low power electronics cooling [8, 9].

Wait et al. further investigated the basic differences between piezoelectric and rotary fans, comparing airflow velocity and turbulence, and highlighting the importance of frequency and amplitude to performance [10]. This focus on operational parameters is reflected in the work of Raman et al. who looked specifically at acoustic signa-tures. The study confirmed that these fans are an ideal choice for quiet environments and ultra-low noise levels (affected by vibration settings) [11]. Transitioning from acous-tics to structural integrity, Zhou et al. showed that multilayer piezoelectric actuators can significantly improve both mechanical strength and vibration amplitude, thus demonstrating the advantages of composite designs [12].

Li et al. used a combination of Finite Element Method (FEM) and Computational Fluid Dynamics (CFD) to map airflow and heat dissipation to better predict performance before the manufacturing stage [13]. These modelling insights provide the basis for the versa-tile applications proposed by Hu et al., who have highlighted

the potential of piezoelectric fans in fields ranging from biomedical instruments to microelectronics, particularly in the ever more crowded market of portable devices [14].

The study of Açıkalın et al. looked to determine the variables behind fan efficiency. The authors' results indicate a subtle role of the technology: piezoelectrically driven fans may not completely replace conventional rotary fans but can be highly effective supplemental components [15]. Moreover, the synergy of experimental data and CFD simulations in their work elucidates the intricate relation between fan location and heat source behaviour [16].

Few studies have examined the driver circuits for these fans. Yong and Fleming developed integrated driver circuits for piezoelectric fans and proposed solutions to enhance efficiency [17].

Wait et al. identified the natural frequency as the critical threshold for achieving peak electromechanical coupling in piezoelectric fans. However, the scope of their power loss evaluation was somewhat restricted by a lack of detail on the circuit's passive components (resistors, inductors, and capacitors) suggesting that a more detailed electrical analysis is still needed [18].

Through the optimization of radial piezoelectric magnetic fans (RPMFs), Abdul Razak et al. explored how geometry and magnet placement determine thermal success. Their study reported an 8.07% improvement in heat transfer and a 7.6% reduction in thermal resistance [1]. This research underscores the importance of magnetic and structural cooperation in next generation fan design.

Figure 1 outlines the procedural steps followed in this study.

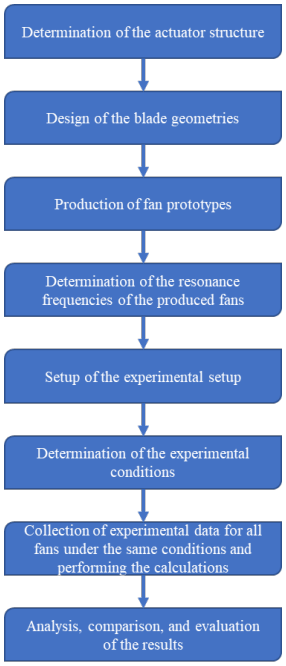

Figure 1. The experimental procedure used in the study

2. Materials and methods

Piezoelectric materials convert electrical energy into mechanical energy when a voltage is applied and, conversely, convert mechanical energy into electrical energy. A piezoelectric fan typically comprises a piezoelectric actuator coupled to a blade structure fabricated from metal or another material.

The components of a typical piezoelectric fan are illustrated in Figure 2.

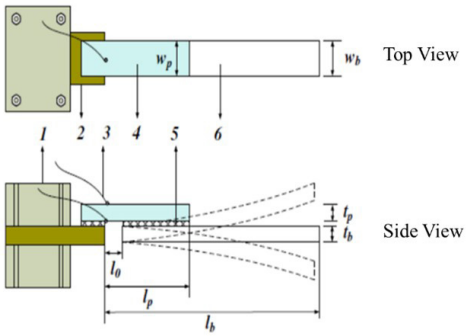

1. Fixture
2. PCB Circuit
3. Conductor Connection Line
4. Piezoelectric Actuator
5. Bonding Surface
6. Blade

Figure 2. General appearance and components of a typical piezoelectric fan [4, 19]

In this study, a three-layer composite bending actuator was used. For the preparation of the outer layers PZT-4 ceramic were used and opted for either copper or bronze (both chosen for their high conductivity) as the substrate material. The Layer configuration of the piezoelectric actuator used in the study is detailed in Figure 3.

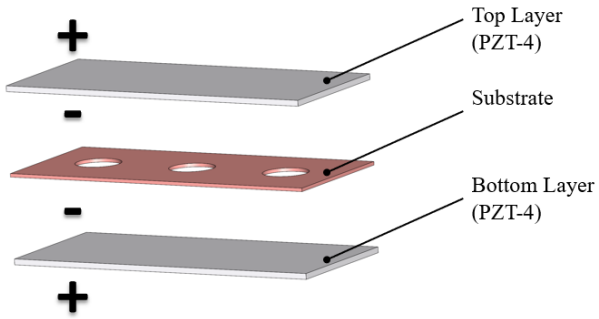

Figure 3. Layer configuration of the piezoelectric actuator used in the study

The geometric modelling and dimensional references used for the piezoelectric fan design were based on the work conducted by A. Hale and X. Jiang [20]. The primary objective of using a three-layer

bending actuator, rather than a conventional single-layer actuator, was to encompass the full production cycle, from ceramic powder to finished product, and to observe the behaviour of a less commonly used structure.

The thicknesses of the PZT-4 ceramic, the intermediate layer, and a third layer were 0.5 mm, 0.3 mm, and 0.5 mm, respectively, giving a total actuator thickness of 1.3 mm. Except for thickness, all actuator components were modelled with identical dimensions of 12.70 mm × 28.00 mm.

For the fan blade geometries, the designs proposed by C. Lin, J. Jang, and J. Leu [21] were taken as reference. As shown in Figure 4, four blade geometries were modelled, each with two base materials, resulting in a total of eight unique blade configurations.

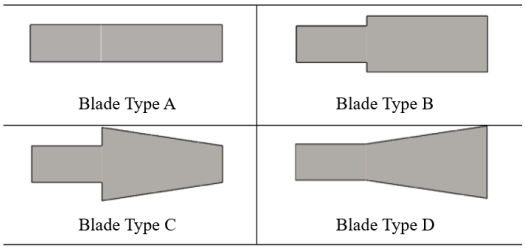

Figure 4. Blade geometry types

The dimensional specifications for the blade designs are presented in Figure 5.

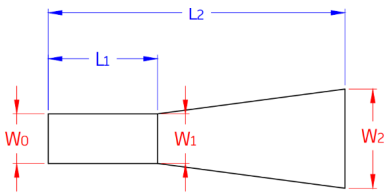

	Blade Type A	Blade Type B	Blade Type C	Blade Type D
L1	28mm	28mm	28mm	28mm
L2	76mm	76mm	76mm	76mm
W0	12.7mm	12.7mm	12.7mm	12.7mm
W1	12.7mm	19.5mm	25.4mm	12.7mm
W2	12.7mm	19.5mm	12.7mm	25.4mm
W1/W2	1	1	0.5	2
t	0.3mm	0.3mm	0.3mm	0.3mm

Figure 5. Dimensional details of the blade structures

The integration of the actuator and the blade structures was modelled as illustrated in Figure 6, and the piezoelectric fans were fabricated accordingly.

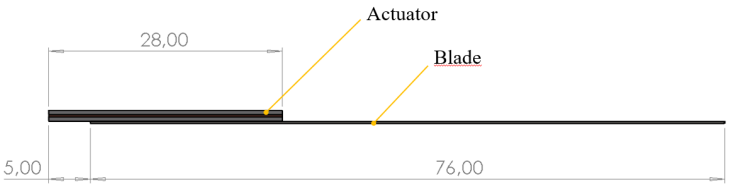

Figure 6. Assembly of the subcomponents of the piezoelectric fan

The resulting fan configurations created within the scope of this study are listed in Table 1.

Table 1. Piezoelectric fan geometries.

Geometry Number	Substrate Material	Blade Material	Blade Type
Geometry #1	Copper	St. Steel	Type A
Geometry #2	Copper	St. Steel	Type B
Geometry #3	Copper	St. Steel	Type C
Geometry #4	Copper	St. Steel	Type D
Geometry #5	Bronze	St. Steel	Type A
Geometry #6	Bronze	St. Steel	Type B
Geometry #7	Bronze	St. Steel	Type C
Geometry #8	Bronze	St. Steel	Type D
Geometry #9	Copper	PVC	Type A
Geometry #10	Copper	PVC	Type B
Geometry #11	Copper	PVC	Type C
Geometry #12	Copper	PVC	Type D
Geometry #13	Bronze	PVC	Type A
Geometry #14	Bronze	PVC	Type B
Geometry #15	Bronze	PVC	Type C
Geometry #16	Bronze	PVC	Type D

All produced fan configurations were subjected to identical test procedures. Since each fan featured a different combination of blade material and geometry, they each possessed a distinct natural resonance frequency. Identifying these frequencies was a critical first step, as they dictate the vortex formation at the blade tips. Before starting the experiments, impedance scanning method for pinpointing these values were used. The measurements fell within the 10–150 Hz range, which aligns with the frequencies typically reported for PVC and stainless-steel blades in the literature [20].

To ensure fair comparison, each fan was operated at its first natural resonance frequency with a fixed input voltage of 288 Vpp.

The experimental setup is shown in Figure 7. Each piezoelectric fan was mounted on a holder and positioned opposite a heat sink whose temperature was raised by an integrated resistor. A temperature sensor, embedded in the heat sink, was used to monitor the cooling effect induced by the fan. All components were enclosed within a 250 mm × 250 mm × 200 mm plexiglass box to minimize the influence of ambient conditions.

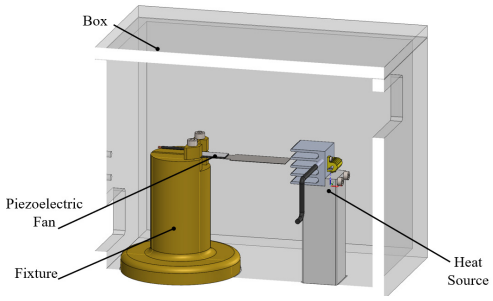

Figure 7. CAD model of the experimental setup

An integrated system was developed to provide power to the fans and the heating element and to monitor temperature variations. A 3D model of the heat source and auxiliary components is shown in Figure 8.

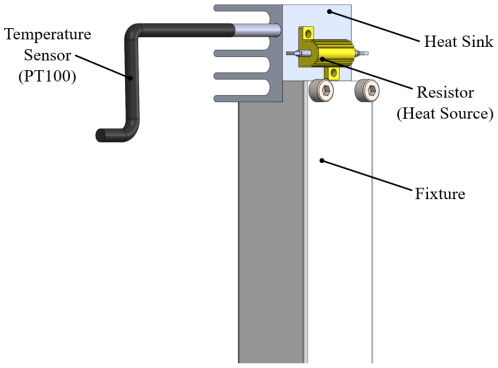

Figure 8. 3D CAD model of the heat source and auxiliary components in the experimental setup

A schematic representation of the of the experimental setup is given in Figure 9.

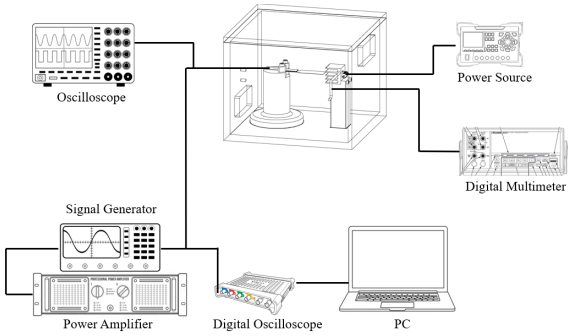

Figure 9. Schematic diagram of the experimental setup

The design of the experimental setup was inspired by similar test systems developed in studies by C.N. Lin [22].

The electronic components used in the experiments are as follows:

- Precision Multimeter: Fluke 8846A
- Temperature Sensor: Jumo Pt100 RTD
- Signal Generator: Rigol DG4102
- Power Amplifier: Crest Audio CA12
- Digital Oscilloscope: PicoScope 5000D
- Differential Probe: Pico TA041
- DC Power Supply: Rigol DP831
- Oscilloscope: R&S RTM3004

A visual representation of the experimental setup using these components is shown in Figure 10.

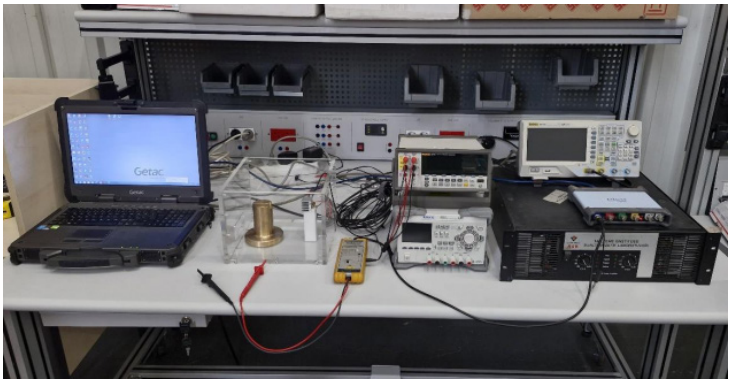

Figure 10. Experimental setup used in the study

The first natural resonance frequencies of the piezoelectric fan geometries were measured and are listed in Table 2. These values were determined via impedance analysis using Equation (1) to compute the resonance frequency:

$$f_0 = \frac{1}{2\pi\sqrt{LC}} \quad (1)$$

where f_0 is the resonance frequency (Hz), L is the inductance (H), and C is the capacitance (F).

Table 2. Measured resonance frequencies of the fan geometries.

Geometry Number	Rezonance Frequency (Measured - Hz)
Geometry #1	91.10
Geometry #2	74.00
Geometry #3	95.40
Geometry #4	71.30
Geometry #5	90.00
Geometry #6	82.00

Geometry #7	93.50
Geometry #8	68.90
Geometry #9	28.20
Geometry #10	25.80
Geometry #11	30.10
Geometry #12	22.60
Geometry #13	22.30
Geometry #14	23.90
Geometry #15	28.40
Geometry #16	22.10

All fans were driven at 288 Vpp using the resonance frequency values listed above. The signal generator and the amplifier ensured that each fan received the required input.

Figure 11 shows a photograph of the experimental test conducted using Geometry 6.

Figure 11. Test photograph of geometry 6

Each experiment began by heating the heat sink to a stable temperature range of 50–55 °C representative of typical electronic component operation temperatures [23]. This initial temperature T0 was recorded, and the fan was operated for 300 seconds. The final temperature T1 was then measured. The temperature drop ΔT was calculated using Equation (2). All temperatures are in degrees Celsius.

$$\Delta T = T_0 - T_1 \quad (2)$$

The apparent power consumption of the system, used to maintain the heat sink at the set temperature, was 4.616 W. The voltage required to maintain this condition ranged from 3.6 to 4 V.

The apparent power consumed by each fan was monitored with an oscilloscope and calculated using Equation (3):

$$S = IxV \quad (3)$$

where I is the current and V is the voltage applied.

3. Results and discussion

Identical experiments were conducted for all 16 piezoelectric fan geometries, and the results are summarized in Table 3.

The apparent power values shown were measured consistently throughout the experiments and remained unchanged during each test.

Table 3. Apparent power and temperature difference values measured for each fan geometry.

Geometry Number	Apparent Poweri (Measured - mW)	ΔT [°C]
Geometry #1	24.35	3.00
Geometry #2	22.42	5.60
Geometry #3	28.28	1.84
Geometry #4	32.56	6.78
Geometry #5	27.86	4.49
Geometry #6	22.64	9.89
Geometry #7	31.47	3.92
Geometry #8	21.61	2.92
Geometry #9	19.44	2.04
Geometry #10	18.35	2.11
Geometry #11	13.86	0.97
Geometry #12	13.52	1.56
Geometry #13	13.85	1.10
Geometry #14	14.50	0.70
Geometry #15	15.54	0.64
Geometry #16	17.11	0.19

As shown in Table 3, the fan labelled Geometry 6 exhibited the highest temperature drop (ΔT=9.89°C), making it the most effective configuration in this study.

Experimental observations indicated that applying an appropriate voltage at the resonance frequency resulted in the highest heat removal when using the Type-B stainless steel blade geometry. Additionally, actuators with bronze as the intermediate layer outperformed those with copper, suggesting that material selection in the actuator significantly affects cooling performance.

Our observation of higher efficiency of stainless-steel blades with gradual widening compared to other geometries is consistent with Lin et al. who showed that widening geometries increase the vortex intensity and convective heat transfer zones [21]. In addition, the better performance of bronze-based actuators than the copper is consistent with the results of Xu et al., which also showed that multi-layer actuators with high stiffness can achieve larger vibration amplitudes [12].

Although Geometry 3 was constructed using stainless steel, it performed significantly worse than the power consumption of 28.28 mW, as it could only reduce the temperature by 1.84°C. This inconsistency indicates possible manufacturing defects, maybe improper bonding between the actuator layers or slight mechanical misalignments during the assembly phase. Such issues could easily lead to undesired residual stress or increased contact resistance, thus hindering the overall efficiency of the piezoelectric fan.

Figure 12 illustrates the relationship between the apparent power input, and the temperature difference achieved over 300 seconds for each geometry operating at resonance.

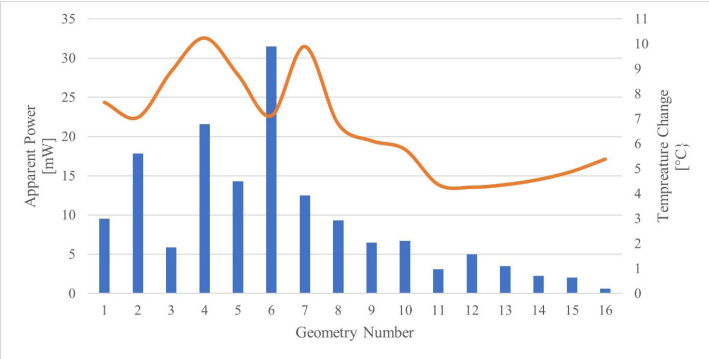

Figure 12. Apparent power vs. temperature difference for all piezoelectric fan geometries.

Apparent power values are indicated by the orange-colored spline in this figure, and temperature change by the navy columns.

The accuracy of our apparent power measurements is limited by the precision of the digital oscilloscope, and the current and differential probes. These variables are defined by computing the overall measurement uncertainty systematically as given below in Equation (4):

$$\text{Uncertainty}(u_s) = S \times \sqrt{\left(\frac{u_V}{V}\right)^2 + \left(\frac{u_I}{I}\right)^2} \quad (4)$$

Where:

Uncertainty of the apparent power (u_S)

Uncertainty of the differential probe (u_V): 0.1V

Uncertainty of the current probe (u_I): 6.4×10^{-4}

With using this formula, the total uncertainty in apparent power measurements was calculated as 0.0220 mVA.

Temperature values during the experiments were measured using a temperature sensor connected to a precision multimeter. The overall uncertainty of temperature measurements was calculated using Equation (5):

$$\text{Uncertainty}(\Delta T) = \sqrt{(\Delta x_1)^2 + (\Delta x_2)^2} \quad (5)$$

Where:

Uncertainty of the temperature sensor (Δx_1): 0.2°C

Uncertainty of the precision multimeter (Δx_2): 0.11°C

The total uncertainty of the temperature measurement was obtained as 0.21°C.

The superior performance of stainless-steel blades was attributed to several factors:

Thermal Conductivity: Stainless steel has a thermal conductivity of about 16.2W/(m.K) [23] while PVC has a thermal conductivity of about 0.17 W/(m.K) [24]. Stainless steel has a much higher conductivity (almost 100 times higher) so it will absorb heat from the environment faster and transfer heat to the air more efficiently.

Material stiffness: At hight vibration frequencies, the stiffness of the blade material, (determined by Young's modulus), plays a critical role in cooling efficiency. Since vibration frequency is inversely proportional to mass, increased material density reduces the resonance frequency. A comparison of mechanical properties is presented in Table 4.

Table 4. Comparison of density and Young's modulus for stainless steel and PVC [24, 25].

	Stainless Steel	**PVC**
Density (ρ) [kg/m3]	**8000**	1380
Young's Modulus (E) [GPa]	**193**	2.6

The superior stiffness and density of stainless steel contributed to higher airflow velocity and, hence, better cooling performance.

Among the stainless-steel based fans, Geometry 6 outperformed the others. The performance gains are likely a result of the blade's widening profile, which not only directs the airflow more effectively but also maximizes the surface area available for cooling. Like blade types B and D, this geometry is critical for improving convective heat transfer. The widening structure ensures a more intensive displacement of heat by encouraging vortex formation and turbulence (or flow mixing) at the blade tips.

The results show good agreement with the existing literature for the blade geometry-flow interaction. For example, Lin et al. [21] showed that the strong vortices and strong convective zones we observed are due to a widening blade profile, mainly due to better mixing of the flow at the tips. This geometric advantage is further improved with material selection. As pointed out by Liu et al. [19], due to the

intrinsic stiffness and thermal conductivity of stainless steel, larger airflow velocity is generated. It is this combination of factors that consistently gives our stainless-steel configurations superior performance to polymer-based alternatives.

While our study confirms that the rigidity and density of stainless steel maximize fan performance, commercial adoption often requires a compromise. The primary concern with metal blades in the field is the risk of electrical interference or short circuiting in dense electronic assemblies. This explains why polymer-based blades remain the industry standard for most consumer electronics they provide a necessary layer of insulation that metal simply cannot offer, despite the marginal reduction in cooling efficiency.

Existing research into blade shapes supports these results, particularly regarding how geometries that widen progressively can trigger more aggressive turbulence and wider cooling areas. The effectiveness of this design is shown in Figure 13, which provides a comparative look at flow structures from prior studies in the field.

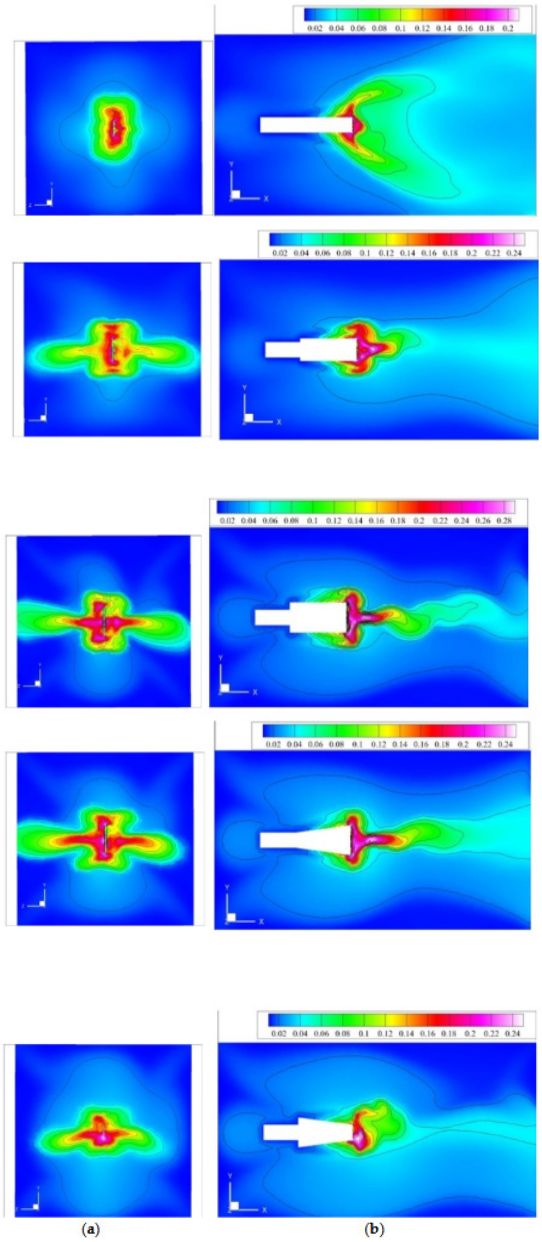

Figure 13. Turbulence intensity vs. blade geometry: **(a)** fan tip plane; **(b)** mid plane of the piezoelectric fan [20]

4. Conclusion

In this study, the cooling performance of piezoelectric fans with various blade geometries and material structures was experimentally evaluated. Three-layer composite bending-type actuators were developed using lead zirconate titanate-4 (PZT-4) ceramic as the active material. Two different materials, bronze and copper, were used for the intermediate actuator layers. To evaluate performance across different materials, we bonded these actuators to blades made from both stainless steel and PVC. By applying this approach to four distinct blade geometries, we successfully developed a suite of 16 fan prototypes for the testing phase.

After identifying the primary resonance frequency for each fan, all units were operated at 288 Vpp to ensure peak performance. To maintain consistency, each fan was subjected to a 300 second testing cycle over a stabilized heat source. Throughout these intervals, the thermal data to evaluate the comparative efficiency of each configuration was recorded.

The experimental data confirms that both the material composition and the structural shape of the blade are focal to fan performance. Specifically, the stainless-steel version of Geometry 6 (with expanding width of fan blade) outperformed all other prototypes. It achieved a large temperature drop of 9.89°C, demonstrating the usefulness of combining high stiffness materials with widening geometries. This performance is attributable to the high thermal conductivity and Young's modulus of stainless steel and to the aerodynamic advantages of the blade geometry.

Moreover, using bronze as the intermediate layer in the actuator yielded better performance than using copper as the intermediate layer. It is attributed that these results to the mechanical properties of the substrate layers. Specifically, the higher elastic modulus of bronze enables larger vibration amplitudes, thereby increasing the fan's volumetric flow rate. In contrast, copper's mechanical profile can actually reduce these amplitudes, even though its thermal conductivity ensures a more uniform heat dissipation. These physical trends were occasionally obscured by performance outliers, which we suspect were caused by the inherent variability of hand assembling the piezoelectric layers.

The Geometry 3, with a power consumption of 28.28 mW and a co-oling effect of only 1.84°C, was one of the least efficient in the study. This poor performance points to integration issues such as residual stress trapped during bonding process or increased contact resistance. Such manufacturing related inconsistencies can greatly limit the mechanical output of the piezoelectric layers.

Geometry 6 came out as the clear frontrunner while other designs struggled with efficiency. It was able to provide peak cooling performance, while consuming only a very low amount of power, 22.64 mW. This unique balance makes it the most energy efficient option among all the stainless-steel configurations we tested.

Acknowledgements

This article is derived from the M.Sc. thesis entitled "Farklı Yapılarda Oluşturulan Piezoelektrik Fanların Verimliliklerinin Karşılaştırılması (Comparison of Efficiency of the Piezoelectric Fans Which Built in Different Configurations- Thesis No: 915344) " completed by author Mehmet Onat MORMENEKŞE at Marmara University / Institute of Science and Technology, in 2024.

References

[1] Abdul Razak, M.A., Taib, M.Y., Zainal, M.R.M., Ali, A.M.M., & Ali, S.A.M. (2023). Design and optimization of radial piezoelectric magnetic fan (RPMF) for thermal management system. Thermal Science and Engineering Progress, 40, 101689. DOI: 10.1016/j.tsep.2023.101689

[2] Yang Y, Chen Z, Kuai Q, Liang J, Liu J, Zeng X. Circuit Techniques for High Efficiency Piezoelectric Energy Harvesting. Micromachines. 2022; 13(7):1044 DOI: 10.3390/mi13071044

[3] Kimber, M., Suzuki, K., Kitsunai, N., Seki, K., & Garimella, S.V. (2009). Pressure and flow rate performance of piezoelectric fans. IEEE Transactions on Components and Packaging Technologies, 32(4),766–775. DOI: 10.1109/TCAPT.2008.2012169

[4] Uç, E. (2018). Fin optimization in a flow field created using a piezoelectric fan (Master's Thesis). Hacettepe University, Institute of Science and Engineering, Ankara, Turkey.

[5] Wang, Q.M., Deng, X.H., Xie, B.M., & Cross, L.E. (1999). Electromechanical coupling and output efficiency of piezoelectric bending actuators. IEEE Transactions on Ultrasonics, Ferroelectrics, and Frequency Control, 46(3),638–646. DOI: 10.1109/58.764850

[6] Physik Instrumente GmbH. (n.d.). Displacement Modes of Piezo Actuators. Retrieved from https://www.physikinstrumente.com/en/expertise/technology/piezo-technology/properties-piezo-actuators/ displacement-modes

[7] Toda, M., & Osaka, S. (1979). Vibrational fan using the piezoelectric polymer PVF2. Proceedings of the IEEE, 67(8),1171–1173. DOI: 10.1109/proc.1979.11419

[8] Kimber, M., Garimella, S.V., & Raman, A. (2007). Local heat transfer coefficients induced by piezoelectrically actuated vibrating cantilevers. International Journal of Heat and Mass Transfer, 50(21–22),4286–4298. DOI: 10.1115/1.2740655

[9] Kimber, M., & Garimella, S.V. (2009). Measurement and prediction of the cooling characteristics of miniaturized piezoelectric fans. International Journal of Heat and Mass Transfer, 52(19–20),4470–4478. DOI: 10.1016/j.ijheatmasstransfer.2009.03.055

[10] Bowen, C., Giddings, P., Salo, A. & Kim, H A. (2011). Modeling and characterization of piezoelectrically actuated bistable composites. Ultrasonics, Ferroelectrics and Frequency Control, IEEE Transactions on. DOI: 0.1109/TUFFC.2011.2011

[11] Açıkalın, T., Raman, A., & Garimella, S. V. (2003). Two-dimensional streaming flows induced by resonating, thin beams. The Journal of the Acoustical Society of America, 114(4), 1785-1795. DOI: 10.1121/1.1610453

[12] Zhou, X., Wu, S., Wang, X., Wang, Z., Zhu, Q., Sun, J., Huang, P., Wang, X., Huang, W. & Qianbo, lu. (2024). Review on piezoelectric actuators: materials, classifications, applications, and recent trends. Frontiers of Mechanical Engineering. 19. DOI: 10.1007/s11465-023-0772-0

[13] Zhe Li, Xing-Rong Huang, Le Fang,Numerical modeling of fluid–structure–piezoelectric interaction for energy harvesting,Computer Methods in Applied Mechanics and Engineering,Volume 414,2023,116164,ISSN 0045-7825, DOI: 10.1016/j.cma.2023.116164.

[14] S.F. Sufian, M.Z. Abdullah, J.J. Mohamed, Effect of synchronized piezoelectric fans on microelectronic cooling performance,International Communications in Heat and Mass Transfer, Volume 43, 2013, Pages 81-89, ISSN 0735-1933, DOI: 10.1016/j.icheatmasstranfer.2013.02.013

[15] Kim, Yong-Hwan & Wereley, Steven & Chun, Chung-Hwan. (2004). Phase-resolved flow field produced by a vibrating cantilever plate between two endplates. Physics of Fluids. 16. 145-162. DOI: 10.1063/1.1630796

[16] Acikalin, T., Wait, S., Garimella, S.V., & Raman, A. (2004). Experimental investigation of the thermal performance of piezoelectric fans. CTRC Research Publications. DOI: 10.1080/01457630490248223

[17] Yong, Y.K., & Fleming, A.J. (2015). Piezoelectric actuators with integrated high-voltage power electronics. IEEE/ASME Transactions on Mechatronics, 20, 611–617. DOI: 10.1109/TMECH.2014.2311040

[18] [18] Wait, S.M., Basak, S., Garimella, S.V., & Raman, A. (2007). Piezoelectric fans using higher flexural modes for electronics cooling applications. IEEE Transactions on Components, Packaging and Manufacturing Technology, 30(1),119–128. DOI: 10.1109/TCAPT.2007.892084

[19] Liu, S.F., Huang, R.T., Sheu, W.J., & Wang, C.C. (2009). Heat transfer by a piezoelectric fan on a flat surface under horizontal/vertical arrangements. International Journal of Heat and Mass Transfer, 52(11–12),2565–2570.DOI: 10.1016/j.ijheatmasstransfer.2009.01.013

[20] Hales, A., & Jiang, X. (2018). A review of piezoelectric fans for low energy cooling of power electronics. School of Engineering and Materials Science, Queen Mary University of London. DOI: 10.1016/j.apenergy.2018.02.014

[21] Lin, C., Jang, J., & Leu, J. (2016). A study of an effective heat-dissipating piezoelectric fan for high heat density devices. Energies, 9(1),1–16. DOI: 10.3390/en9080610

[22] Lin, C.N. (2013). Heat transfer enhancement analysis of a cylindrical surface by a piezoelectric fan. Applied Thermal Engineering, 50(1),693–703. DOI: 10.1016/j.applthermaleng.2012.07.023

[23] Sayyed, J, Nabeel, A., & Firdaus, Ansari. (2025). Exploring Thermal Conductivity: Experimental Insights Into Heat Transfer Properties Of Common Materials. International Journal of Environmental Sciences. 11. DOI: 10.64252/5sxkbj63

[24] Thyssenkrupp Materials UK. (n.d.). Stainless Steel 304 Material Data Sheet. Retrieved from https://www.thyssenkrupp-materials.co.u k/sta-inless-steel-304-14301.html

[25] Smiths Advanced Metals. (n.d.). PVC-U Material Data Sheet. Retrieved from https://www.smithmetal.com/pdf/plastics/pvc-u.pdf